Local Reactivity of Charybdotoxin, a K^+ Channel Blocker

Joel Ireta,[†] Marcelo Galván,*[,†] Kyeonjgae Cho,[‡,§] and John D. Joannopoulos[‡]

Contribution from the Departamento de Química, División de Ciencias Básicas e Ingeniería, Universidad Autónoma Metropolitana—Iztapalapa, A.P. 55-534, México D.F. 09340, and Department of Physics, Massachusetts Institute of Technology, Cambridge, Massachusetts 02139

Received October 31, 1997. Revised Manuscript Received July 6, 1998

Abstract: Charybdotoxin (ChTX) is a 37-residue polypeptide that has been extensively used in site-directed mutagenesis experiments as a template to deduce models for the external pore appearance of K^+ channels. The microscopic details of the ChTX−channel interaction, however, remain as a challenge for experimental and theoretical approaches. In this work, regional charge-transfer abilities, measured by chemical softness, $s(\mathbf{r})$, are used as companion properties of the electrostatic potential, $V(\mathbf{r})$, in the search for a qualitative structure−function relationship in the ChTX−K^+ channel interaction. Both quantities were obtained with an ab initio methodology in massively parallel computers. In the analysis of $s(\mathbf{r})$ and $V(\mathbf{r})$, regions of the size of amino acids were considered because this is the appropriate scale to correlate with site-directed mutagenesis experiments. The correspondence between experimentally identified crucial amino acids sites and regional softnesses indicates that charge transfer to ChTX could be one of the main stabilization effects in the ChTX−channel complex. Also, it provides an explanation for the strong dependence of the dissociation constant of the complex on mutations of crucial amino acids. In addition, it is shown to be feasible to find structure−function relationships by combining local reactivity parameters and experimental data involving site directed mutagenesis.

Introduction

Charybdotoxin (ChTX) is a 20 Å × 20 Å × 25 Å globular polypeptide formed by a three-turn α helix lying on a small three-strand antiparallel β sheet. As has been pointed out previously,[1−3] it would be difficult to find another molecule that has contributed an equivalent amount to our present knowledge and understanding of ion-channel structure and function. Considering this toxin as a template for channel structure, a model for the ChTX channel receptor has emerged.[4−6] Also, a cluster of eight residues, forming about 25% of the toxin surface, has been identified as the area of intimate contact with the receptor site.[4] A system such as this represents a challenge for the application of local chemical reactivity criteria derived from ab initio electronic structure calculations. Because of its size (ChTX has more than 500 atoms and 1604 valence electrons), it represents a system in the limit of current calculational tractability using ab initio methodologies.[7−9] As a small protein, ChTX is a complex molecule that contains many functional groups with a wide range of chemical environments. In addition, it is not a priori clear what the appropriate scale for the analysis should be. It could be done on an atom-by-atom basis, or by analyzing functional groups, or by analyzing amino acid by amino acid. One of the main objectives of the present work is to characterize the amino acids situated on the active surface of ChTX according to their charge-transfer capacities and their electrostatic interaction abilities. To measure charge-transfer abilities, local chemical softness is used,[10] while calculation of the electrostatic potential itself can account for the electrostatic active areas of the toxin. Both quantities were determined ab initio within the framework of density functional theory methodologies.[7] Because of the size of the molecular system, massively parallel computation was needed. The scope of this work includes the description of the density of states of ChTX, to identify the bands that are formed because of the polymeric nature of the molecule.

Computational Method

The electronic structure of ChTX was obtained by total energy pseudopotential calculations (TEPC).[7] The geometry of the toxin was taken from recently reported NMR experiments.[11,12] In the TEPC methodology, the core electrons are substituted by a nonlocal atomic pseudopotential designed, in our case, by a procedure developed by Rappe et al.[13,14] and tested in small molecules.[15] The use of supercells to treat isolated molecules within the framework of TEPC has been

[†] Universidad Autónoma Metropolitana—Iztapalapa.
[‡] Massachusetts Institute of Technology.
[§] Present address: Mechanics and Computation Division, Mechanical Engineering Department, Stanford University, Stanford, CA 94305.

(1) Miller, C. *Science* **1991**, *252*, 1092.
(2) García, M. L.; Knaus, H. G.; Munujos, P.; Slaughter, R. S.; Kaczorowski, G. J. *Am. J. Physiol.* **1995**, *269*, C1.
(3) Miller, C. *Neuron* **1995**, *15*, 5.
(4) Stampe, P.; Kolmakova-Partenski, L.; Miller, C. *Biochemistry* **1994**, *33*, 443.
(5) Hidalgo, P.; MacKinnon, R. *Science* **1995**, *268*, 307.
(6) Aiyar, J.; Withka, J. M.; Rizzi, J. P.; Singleton, D. H.; Andrews, G. C.; Lin, W.; Boyd, J.; Hanson, D. C.; Simon, M.; Dethlefs, B.; Lee, C.; Hall, J. E.; Gutman, G. A.; Chandy K. G. *Neuron* **1995**, *15*, 1169.
(7) Payne, M. C.; Teter, M. P.; Allan, D. C.; Arias, T. A.; Joannopoulos, J. D. *Rev. Mod. Phys.* **1992**, *64*, 1045.
(8) Challacombe, M.; Schwegler, E. *J. Chem. Phys.* **1997**, *106*, 5526.
(9) Strain, M. C.; Scuseria, G. E.; Frisch, M. J. *Science* **1996**, *271*, 51.
(10) Parr, R. G.; Yang, W. *Density Functional Theory of Atoms and Molecules*; Oxford University Press: New York, 1989; pp 101−104.
(11) Bontems, F.; Roumestand, C.; Gilquin, B.; Ménez, A.; Toma, F. *Science* **1991**, *254*, 1521.
(12) In this work, one of the 12 structures reported in ref 11 was used.
(13) Rappe, A.; Rabe, K.; Kaxiras, E.; Joannopoulos, J. D. *Phys. Rev. B* **1990**, *41*, 1227.
(14) Rappe, A.; Joannopoulos, J. D. In *Computer Simulations in Material Science*; Meyer, M., Pontikis, V., Eds.; NATO ASCI Series 204; Kluwer Academic: Dordrecht, 1991; p 409.
(15) Ireta, J.; Galván, M. *J. Chem. Phys.* **1996**, *105*, 8231.

S0002-7863(97)03762-1 CCC: $15.00
Published on Web 09/11/1998

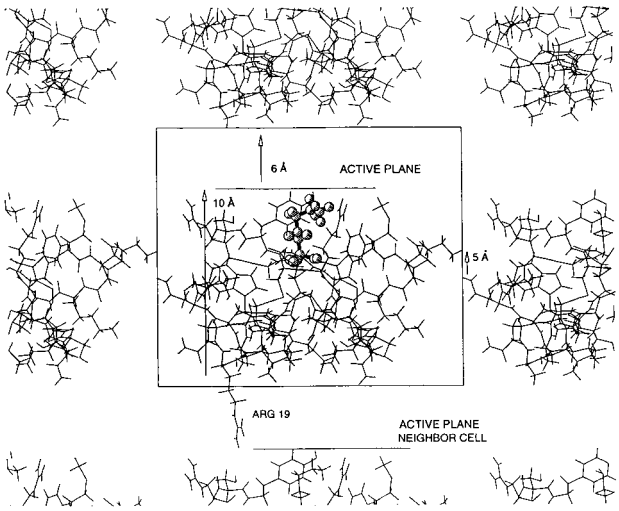

Figure 1. Side view of the unit cell used in the calculation of ChTX. It shows the neighbor cells and the shortest distance between atoms in vicinal cells along two directions. The vacuum above the plane containing the crucial amino acids Ser10, Trp14, Arg25, Lys27, Met29, Arg34, and Tyr36 is at least 6 Å wide. Also, Arg19, which was changed for Ala in the calculation, is indicated to emphasize that it points toward the active plane of the toxin in the neighbor cell on the bottom. Indeed, the change from Arg19 to Ala19 reduces substantially the size of the unit cell, and it decreases the size of the wave function about 20%. Lys27 is shown in ball-and-stick representation in order to have a reference point.

tested for several groups;[15−18] in the present work, this supercell is 29.1 Å × 24.62 Å × 28.53 Å. This size falls within the criterion introduced by Rappe et al. to describe appropriately isolated molecules[16] (see Figure 1).

The only structural change introduced in our calculations was the replacement of arginine in position 19 with alanine. Arg19 is a charged amino acid, located approximately 10 Å from the active plane of ChTX (see Figure 1). The motivations behind this change will be detailed in what follows. As the calculation of the electronic structure is done under periodic conditions, Arg19 in the original unit cell would be close to the active surface of the toxin in a neighbor cell. The standard procedure to eliminate such spurious interactions involves the use of larger unit cells, but it is well-known that, for charged systems, it is harder to reduce these effects because of the long-range nature of Coulombic interactions.[19] Therefore, replacing a charged amino acid with a neutral one is a suitable way of bypassing this limitation if, as is known through the use of point mutagenesis, Arg19 is a noncrucial site for ChTX−channel interaction.[4,20,21] In addition, changing arginine to alanine reduces substantially the size of the original unit cell and, consequently, the number of plane waves, a situation that helps to diminish the computational effort.

In the TEPC methodology, there are two aspects that are worth mentioning: the accuracy in the description of the electron−electron interaction and the basis set used to expand the Kohn−Sham orbitals. In relation to the former aspect, we use the exchange and correlation potential within the local density approximation.[22] With respect to the plane waves basis set, a 6 Ry cutoff was used to define it. This is a weak approximation; however, it was found that, at this low cutoff, it is possible to recover many aspects of the electronic structure, as will be discussed in the next section. In addition, we are calculating a system with a net charge of +4. This introduces an error in the total energy inversely proportional to the unit cell volume.[23] The level of theory imposed by the three aspects mentioned bounds our analysis to a qualitative description of the charge-transfer and electrostatic interaction capabilities in the outer regions of the molecule.

Results

Electronic Structure of ChTX. One of the limitations of using TEPC to study biomolecules is that they contain first row atoms. This implies the use of a large energy cutoff to generate their pseudopotentials, a situation that inhibits the study of polypeptides of hundreds of atoms because the number of plane waves in the basis set may grow to hundreds of thousands. Also, the description of localized pieces of the density is a challenge because plane wave basis sets are more suitable to follow the behavior of delocalized states.

To perform calculations in biomolecules with reasonable computational resources, a possible scheme could be the usage of cutoffs lower than those implied in the generation of the pseudopotential. In this work, the pseudopotentials used were generated at 40 Ry cutoff, but the calculations were done at 6 Ry. This aggressive truncation of the basis set produces a tremendous loss of information in regions of high-density values. As was shown for small systems,[15] if the calculations are carried out at 20 Ry cutoff, charge distribution, bond lengths, and vibrational frequencies are quantitatively well described; however, below 10 Ry, the error in the description of those properties rapidly increases. At 6 Ry, the topological characteristics of the charge distribution remain qualitatively well described in regions far from the nuclei, where the electron density has values smaller than 0.5 e/Å^3 (see Figure 6 of ref 15). This behavior was also observed when the charge distribution corresponding to the highest occupied orbitals was analyzed.[24]

By taking care of the limitations mentioned above, the charge density of ChTX obtained at 6 Ry was studied band by band. An unexpected fact is that relevant aspects of the electronic structure of the polypeptide are preserved: the well-known shapes of lone pairs, π clouds, and σ bonds are clearly recognized. To identify the bands formed because of the polymeric nature of the molecule, the density of states, $N(E)$, at the Γ point in the first Brillouin zone is displayed in Figure 2. For comparison, we include $N(E)$ for ChTX, ChTX without the α helix (ChTX β sheet), and cysteine. The shape of $N(E)$ is almost the same for both polypeptides. Also, the comparison of $N(E)$ of both polymers with the eigenvalue distribution of cysteine, a monomer containing the same sample of atoms, indicates that band formation is related to the combination of states of the isolated amino acids in a similar way as atomic states are responsible for band formation in solids. The resemblance of $N(E)$ in ChTX and ChTX β sheet suggests that the general shape of this quantity is independent of the structural motif (α helix or β sheet). Among the filled states, there are three regions in $N(E)$ separated by at least 2 eV; the broadest region, which goes up to the Fermi level, can be further divided in three bands to perform a detailed assignation of these pieces of the electron density. The bandwidths of the five bands are displayed in Table 1. The names used in the table are related to the main features of each portion of the electron density: πlp corresponds to a band in which the main contributions come

(16) Rappe, A.; Joanopoulos, J. D.; Bash, P. A. *J. Am. Chem. Soc.* **1992**, *114*, 6466.
(17) Andrews, S. B.; Burton, N. A.; Hillier, I. H.; Holender, J. M.; Gillan, M. J. *Chem. Phys. Lett.* **1996**, *261*, 521.
(18) Milman, B.; Lee, M. H. *J. Phys. Chem.* **1996**, *100*, 6093.
(19) Jarvis, M. R.; White, I. D.; Godby, R. W.; Payne, M. C. *Phys. Rev. B* **1997**, *56*, 14972.
(20) Park, C.; Miller, C. *Biochemistry* **1992**, *31*, 7749.
(21) Goldstein, S. A. N.; Pheasant, D. J.; Miller, C. *Neuron* **1994,** *12*, 1377.
(22) In the present work, the exchange and correlation potential used was set according to the following reference: Perdew, P.; Zunger, A. *Phys. Rev. B* **1981**, *23*, 5048.
(23) Leslie, M.; Gillian, M. J. *J. Phys. C: Solid State Phys.* **1985**, *18*, 973.
(24) Ireta, J. Master in Sciences Thesis, Universidad Autónoma Metropolitana−Iztapalapa, 1995.

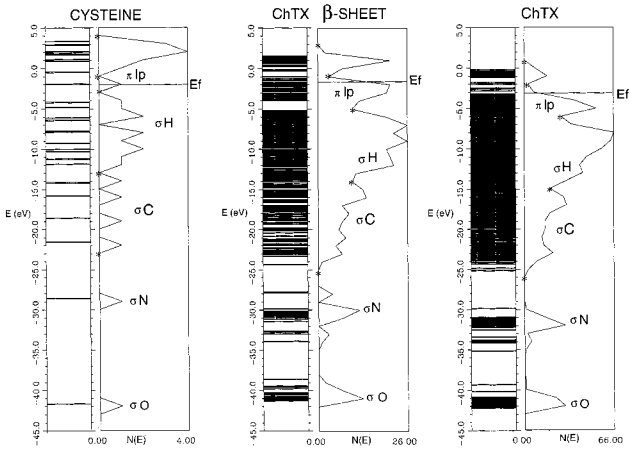

Figure 2. Eigenvalues spectra and density of levels, $N(E)$, for cysteine ($C_3H_7O_1N_1S_1$, 18 occupied states), the β sheet of ChTX ($C_{74}H_{133}O_{22}N_{27}S_7$, 367 occupied states), and ChTX ($C_{173}H_{274}O_{55}N_{54}S_7$, 802 occupied states). Ef indicates the Fermi level, and πlp, σH, σC, σN, and σO are labels for different bands in decreasing order of energy.

Table 1. Characteristic Bandwidths of Charybdotoxin Calculated at 6 Ry

band[a]	polypeptide	bandwidth (eV)
σO	ChTX	2.86
	ChTX−β sheet	2.70
σN	ChTX	5.28
	ChTX−β sheet	6.11
σC	ChTX	10.03
	ChTX−β sheet	10.01
σH	ChTX	8.99
	ChTX−β sheet	9.03
πlp	ChTX	2.76
	ChTX−β sheet	2.19

[a] See text for band identification.

from π clouds of aromatic rings and lone pairs of oxygen, nitrogen and sulfur; σO corresponds to σ-bond-like structures between oxygen atoms and carbon atoms, and σN between nitrogen atoms and carbon atoms; the σC band can be assigned to σ bonds that involve two carbon atoms; and finally, the σH band contains σ bonds in which one of the atoms is hydrogen. The assignations described above are based on the analysis of graphics in which isosurfaces of the density, with values smaller than 0.5 e/Å^3, are plotted on the polypeptide's framework. Figure 3 is an example of this kind of graphics. In this figure, it is evident that all bands represent fractions of the charge density that are spread throughout the polypeptide.

It is important to keep in mind that the use of pseudopotentials avoids the presence of states related to atomic cores. Consequently, even the deepest states are of bonding character. The four deepest bands correspond to σ-like states; the first band (σO) involves oxygen atoms, the next one in energy is related to nitrogen atoms, the third one is related to carbon atoms, and the last one is associated with hydrogen atoms. This trend is consistent with the relative electronegativity of these atoms: electrons are more stable around the atom with larger electronegativity. It is interesting to notice that bandwidths agree with the idea that the broadest band is associated with strong overlap and delocalization.[25] Another point to emphasize is the fact that π states and lone pairs contribute to the greatest extent to build the valence band of the polypeptide; a similar situation is observed in organic molecules, containing the same sample of atoms, in which the highest occupied states are, in general, π states and lone pairs.

The mentioned trends show that the use of TEPC methodology at a very low energy cutoff allows the qualitative description of the electronic structure of polypeptides. This is true only if the analysis is restricted to the external regions of the electronic distribution. In particular, the behavior of localized pieces of the density, whose description is a challenge for plane wave basis sets with a reduced number of elements, follows the chemical and physical intuition.

Electrostatic Potential and Local Softness. As ChTX and the channel are charged species, the main interaction forces can be divided into two types: on one hand, there are long-range electrostatic interactions between the charged regions of the molecules; on the other hand, there should be short-range interactions related with the close contact regions of both macromolecules. The last effect may be related to charge-transfer interactions, and the former is associated with the electrostatic potential.

The upper right panel of Figure 4 shows the electrostatic potential on the active plateau of ChTX. One clearly distinguishes that the positive regions match with the sites of the well-known positively charged residues. This result can be obtained by any simple point charge model. However, if we perform the same analysis at 3 Å rather than at 1.5 Å (see Figure 4c), the positive values of the electrostatic potential around Arg25 almost disappear, indicating that the methodology distinguishes the behavior of two equivalent charged amino acids, Arg25 and Arg34. This suggests that Arg25 is not a good candidate for long-distance electrostatic interactions, in contrast to Lys11, Lys27, Lys31, Lys32, and Arg34.

The close-contact charge-transfer capabilities of ChTX were studied by using the local chemical softness,[26,27]

$$s(\mathbf{r}) = \left(\frac{\partial \rho(\mathbf{r})}{\partial \mu}\right)_{T,v(\mathbf{r})} \approx \frac{1}{\Delta\mu}\int_{\mu}^{\mu+\Delta\mu} \mathrm{d}E g(E,\mathbf{r})$$

In this expression, $\rho(\mathbf{r})$ is the electron density, μ is the chemical potential (Fermi level), T is the temperature, $v(\mathbf{r})$ is the external potential, and $g(E,\mathbf{r})$ is the local density of sates; the approximation represented by the integral is a finite differences scheme that estimates local softness by using the "frontier bands" of the polypeptide. As has been pointed out previously,[10] there are two local softnesses, $s^+(\mathbf{r})$, related to electron transfer from the polypeptide to the channel, and, $s^-(\mathbf{r})$, which measures the charge acceptance capabilities of the toxin. The quantity $\Delta\mu$ is related to the width of the frontier bands of the system.

The concept of local chemical softness has been useful for investigating the intrinsic reactivity of a wide range of systems.[28] This quantity permits the determination of initial attacking points during a reaction process according to the local hard and soft acids and bases principle (HSAB).[29] This principle establishes that "soft regions of a system prefer to interact with soft reactants whereas hard regions will prefer hard species". It is important to mention that the hard−hard interactions are mainly related to long-range electrostatic effects and that soft−soft interactions are driven by short-range charge-transfer effects. In contrast to electron density, which gives information about where the

(25) Hoffmann, R *Solids and Surfaces: A Chemist's View of Bonding in Extended Structures*; VCH Publishers: New York, 1988; pp 7−9.

(26) Yang, W.; Parr, R. G. *Proc. Natl. Acad. Sci. U.S.A.* **1985**, *82*, 6723.

(27) Brommer, K. D.; Galván, M.; Dal Pino, A., Jr.; Joannopoulos, J. D. *Surf. Sci.* **1994**, *314*, 57.

(28) Sen, K. D., Ed. *Chemical Hardness*; Structure and Bonding 80; Springer-Verlag: Berlin, 1993.

(29) Yang, W.; Mortier, W. J. *J. Am. Chem. Soc.* **1986**, *108*, 5708.

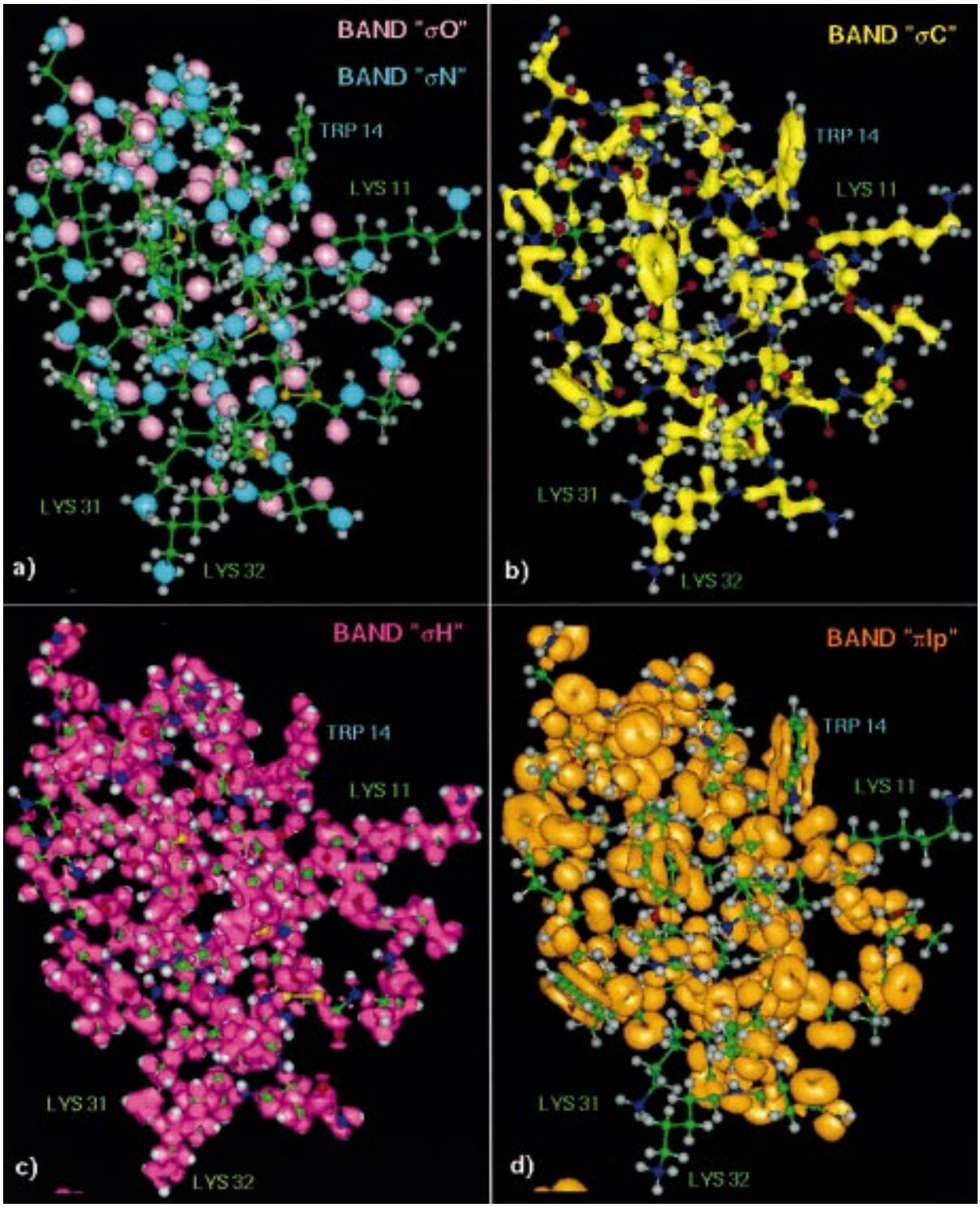

Figure 3. Isosurfaces of the local density of states integrated by band according to Figure 2. Bands σO and σN corresponds to the C−O (pink) and N−C (blue) σ bonds, respectively; the band σC has contributions mainly from C−C (yellow) σ bonds; in the band σH, σ bonds that involve hydrogen atoms prevail (purple); the band πlp, the valence band, is mainly composed by lone pairs of oxygen, nitrogen, and sulfur (orange); also, it includes π clouds of aromatic amino acids. The values of the isosurfaces, in e/Å^3, are 0.50 for σO, σN, and σH; for σC and πlp the values are respectively 0.45 and 0.13.

electrons are, local softness provides an idea of the preferred sites to perform charge-transfer processes.

When $s^+(\mathbf{r})$ is analyzed for ChTX, it is found that there are no special donor capacities related to an extended area of a particular amino acid. Instead, the donor capacity is localized around sulfur atoms on the sulfur bridges and Met29. This strongly suggests that charge transfer from the toxin to the channel cannot be crucial. A different pattern is observed for $s^-(\mathbf{r})$ (see Figure 4d). There are four regions with high capacity to accept charge in the active plane of ChTX. One of them is formed by Lys27, Met29, Arg34, and Tyr36; the second includes Lys31 and Lys32; the third contains Ser10 and Lys11; and the last one contains only Arg25. The back non-interactive site of the toxin has no charge-acceptor regions.

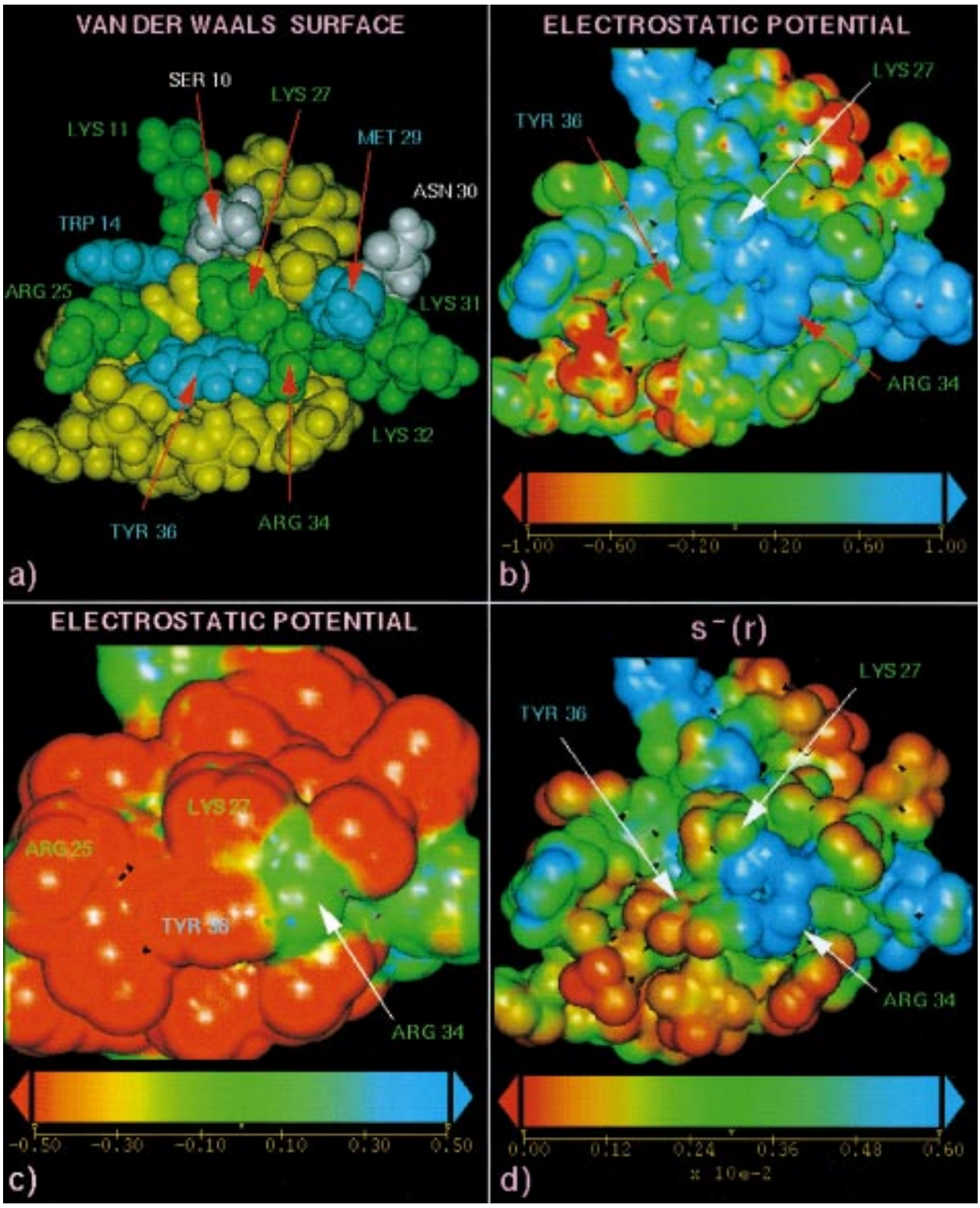

Figure 4. Electrostatic potential and local softnesses for the active plateau of charybdotoxin. The upper left panel displays the relevant amino acids in the interaction with the K^+ channel in a typical van der Waals surface representation. Following Stampe et al.,[4] they are classified as (a) positive charged (in green), Lys11, Arg25, Lys27, Lys31, Lys32, and Arg34; (b) strongly hydrophobic (blue), Trp14, Tyr36, and Met29; and (c) having H-bonding capacity (white), Asn30, Ser10. The other three panels show projections of the electrostatic potential and local softness, $s^-(\mathbf{r})$, onto a surface setup as a superposition of spheres of constant radii. The upper right panel corresponds to the electrostatic potential projected onto spheres of 1.5 Å radius; the lower left panel is a projection of the same property but at 3 Å radius. The lower right panel displays $s^-(\mathbf{r})$ projected onto 1.5-Å spheres; this quantity was calculated with $\Delta\mu = 2.56$ eV.

Discussion

Molecular recognition between macromolecules is a complex process that involves many effects. Among them, the most common are steric interactions, hydrogen bond formation, electrostatic interactions, and hydrophobicity.[30] In addition, to have a complete picture of ChTX−channel interaction requires the knowledge of the structural features of both macromolecules. Until now, only the geometry of ChTX was known. This

information has been useful in deducing some characteristics of the channel vestibule by using ChTX as a probe molecule. As was pointed out in the Introduction, this work, rather than trying to give a complete description of the ChTX−channel interaction, is an attempt to determine if short-range charge-transfer effects play a significant role in such an interaction.

As expected, positively charged amino acids are good electron acceptors, but there are also neutral crucial amino acids having a markedly acceptor character. What is striking is that most of the amino acids associated with the four regions, mentioned above as electron acceptor areas, have been reported as crucial in the activity of the toxin because they alter the kinetics of the ChTX−channel interaction mainly through increasing the dissociation constant, k_{off}, in the reaction[4,20,21]

$$\text{ChTX} + \text{channel} \underset{k_{off}}{\overset{k_{on}}{\rightleftharpoons}} \text{ChTX}-\text{channel}$$

These results indicate that charge transfer to ChTX could be one of the main stabilizing effects in the ChTX−channel complex. Other evidence that supports the idea that charge transfer should be from the channel toward the toxin is the fact that the channel vestibule is mainly negatively charged.[31]

It is interesting to note that the region defined by Lys27, Arg34, Tyr36, and Met29 is the only one exhibiting a combination of high acceptor capacity, strong positive character, and one atom (the S atom in Met29) with electron donor ability. Experimentally, it is known that this region, which is close to the channel mouth and is the most active in reducing k_{off} values upon mutations, plays an important role in understanding the affinity of ChTX for K^+ channels.[3]

There are two other regions, one formed by Lys11, and the other by Lys31 and Lys32 (see Figure 4), where a combination of charged and acceptor character is observed, but they do not affect k_{off}. A possible reason for this behavior is that they are far from the ChTX region, which is in close contact with the channel; another possibility is related to the idea that the channel must have a soft donor site in an appropriate position in order to develop a short-range charge-transfer interaction with the soft acceptor region of ChTX. In fact, experimental results have shown that Lys11 and Lys31 amino acids take part in long-distance interactions;[32] this is in agreement with the analysis of the electrostatic potential previously performed. What is known about the capacity of Lys32 to develop covalent bonds has been determined in its interaction with the β subunit of the high-conductance Ca^{2+}-activated K^+ channel.[33] However, the rationalization of such experiments is more difficult because of the presence of cross-linking reagents.

The analysis of the regional reactivity of ChTX was done with the properties calculated for the isolated molecule. There must be a change in these properties when the molecule is in the presence of a solvent. However, in the case of ChTX−channel interaction, the crucial amino acids influence mainly the dissociation rate constant. Therefore, these amino acids are involved in maintaining the ChTX−channel complex stable through close contact interactions. When the two macromolecules are in close contact, the presence of solvent molecules around the active sites is less probable, and the interaction is determined, to the greatest extent, by the intrinsic properties of the isolated molecules.

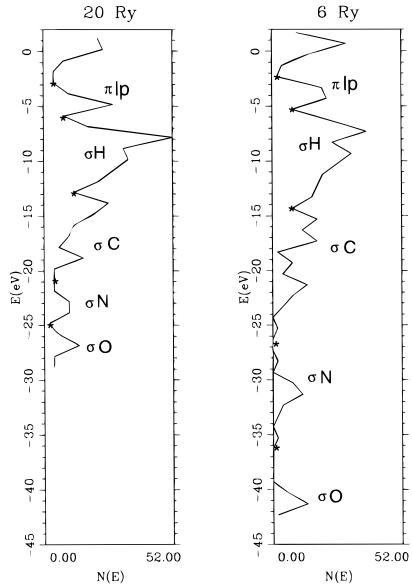

Figure 5. $N(E)$ for a polypeptide ($C_{44}H_{77}O_{11}N_{15}S_1$, 199 occupied states, charge +2) smaller than ChTX β-sheet obtained at 6 and 20 Ry. This polypeptide was built up by exchanging almost all amino acids of the ChTX β sheet with alanine, except the Lys27, Met29, Arg34, and Tyr36. The labels πlp, σH, σC, σN, and σO are equivalent to those of Figure 2.

One might be tempted to say that the lack of charge acceptor capacities on the non-interactive side of the toxin is an indication that one was able to predict the location of the active surface of the toxin without any reference to experimental data. However, this is not a straightforward conclusion, because molecular recognition is a multifaceted issue; furthermore, we introduce a structural change in that region of the molecule. Also, it is important to point out that, to obtain a quantitative structure−function relationship, a systematic study of a series of mutants with a defined tendency in their activities is required. According to the results of this work, by using the theoretical tools currently available and the experimental information at hand, such study for ChTX is feasible.

An important question about the usefulness of low-energy cutoff calculations remains: how many features of the electronic structure described in the Results section will be preserved if a better basis set is used? To address this question, we perform calculations at 6 and 20 Ry on a polypeptide smaller than the ChTX β sheet. As was pointed out in the Results section, a 20 Ry calculation is a good standard to compare the 6 Ry approximation. The comparison of $N(E)$ for these two basis sets is shown in Figure 5. At 6 Ry, the three most bounded bands (σO, σN, and σC) are shifted to lower values of energy as compared to the 20 Ry bands; in contrast, the bands σH and πlp are in similar regions of energy for both cases. In general, the eigenvalues of the unoccupied states at 6 Ry are shifted by a small amount to higher energies. In Figure 6, a comparison of three local quantities calculated at 20 and 6 Ry is displayed. These local quantities are equivalent to those described in the Results section and that are used for the chemical reactivity analysis of ChTX. The two top panels, a and b, show isosurfaces of the charge density corresponding to the highest occupied band (πlp); there are some differences in this band which are more evident around the aromatic ring, but, in general, the resemblance is quite good, considering the big difference between the two basis sets employed in the calculations. It is

(30) Dean, P. M. In *Concepts and Applications of Molecular Recognition*; Johnson, M. A., Maggiora, G. M., Eds.; Wiley-Interscience: Los Angeles, 1990; pp 211−237.
(31) Anderson, C.; Mackinnon, R.; Smith, C.; Miller, C. *J. Gen. Physiol.* **1988**, *91*, 317.
(32) Naini, A. M.; Miller, C. *Biochemistry* **1996**, *35*, 1681.
(33) Munujos, P.; Knaus, H.; Kaczorowski, G. J.; García, M. L. *Biochemistry* **1995**, *34*, 10771.

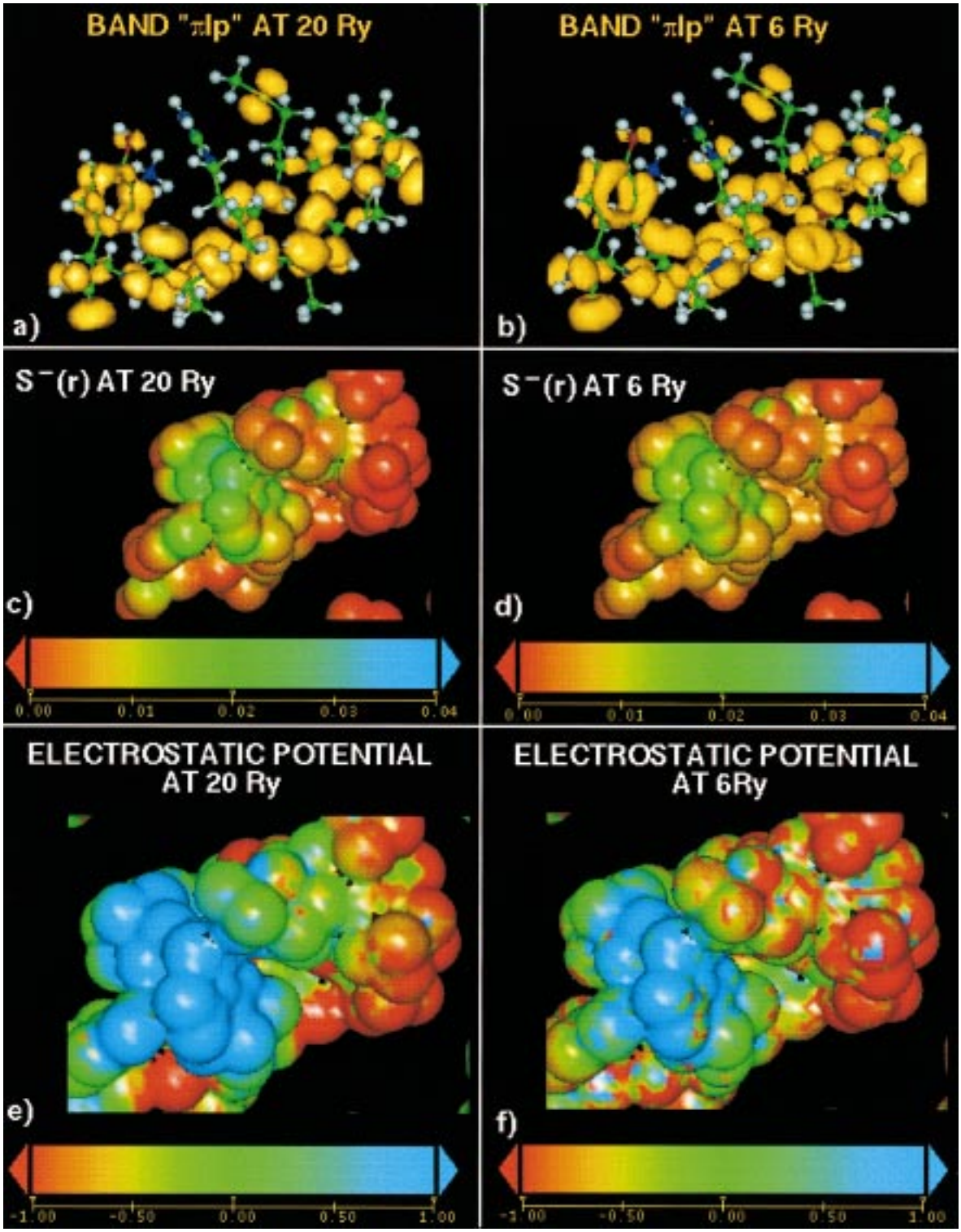

Figure 6. Electronic density of πlp band (panels a and b), local softness, $s^-(\mathbf{r})$, (panels c and d), and electrostatic potential (panels e and f). These properties were calcultated at 6 and 20 Ry for a polypeptide smaller than the ChTX β sheet (see caption of Figure 5). The value of both isosurfaces of the electronic density is 0.13 e/Å^3. The $s^-(\mathbf{r})$ and electrostatic potential are shown as a projection onto a surface of overlapping spheres centered in the nuclei positions. The radius of the spheres is 1.5 Å. Values of $\Delta\mu = 3.71$ eV at 20 Ry and $\Delta\mu = 4.12$ eV at 6 Ry were used to calculate $s^-(\mathbf{r})$, which corresponds to 20 empty states in both cases.

important to notice that the charge density pieces of this band appear in the same regions in space for both calculations, a situation that is also observed for the rest of the bands. The local softness related to the ability of the system to accept charge, $s^-(\mathbf{r})$, is displayed in panels c and d in a projection equivalent to the one used in Figure 4. Again, there are differences, but they do not alter the regions where charge-transfer capabilities are located. Projections of the electrostatic potential are shown in panels e and f. Among the three quantities displayed in Figure 6, the electrostatic potential is the most sensible to the strong truncation of the basis set. At 6 Ry, a contraction of the positive regions is observed, in addition to an expansion of the negative areas. However, this property is still useful to define the orientation of the positive

regions of charged amino acids in ChTX. One can rationalize the effects described above if one recalls that the truncation of a plane wave basis set has more impact in zones where the Kohn−Sham orbitals (and, consequently, the charge density) rapidly change. Therefore, the most localized states will be more affected by the 6 Ry approximation. This is the reason the states around the Fermi level, which are crucial for the chemical reactivity of the system, are qualitatively well described at low cutoff. In summary, as expected, there are changes due to the truncation of the basis set, but, because of the nature of the plane wave basis sets, those changes do not affect strongly the states around the Fermi level. Thus, the qualitative behavior of the local softness is preserved at 6 Ry.

Conclusions

The results obtained in this work demonstrate the usefulness of TEPC methodologies at very low cutoff to achieve qualitative regional charge-transfer capabilities in polypeptides. This analysis can be done if reliable geometries are available. At low cutoffs, only the outer regions of the macromolecular charge density are well described. Yet, these regions are the crucial ones for a chemical reactivity description. Besides, the study of the outer regions is helpful to perform an amino acid-by-amino acid characterization, which is important to correlate with site-directed mutagenesis experiments. The combination of the electrostatic potential and local softness can be used to give a complementary picture (electrostatic and charge transfer) of the complex interaction between macromolecules. Indeed, the results of this work suggest that it is not possible to explain the behavior of ChTX−channel interaction by the exclusive use of electrostatic effects.

Acknowledgment. This work was supported in part by CONACYT through Project No. 400200-5-4875E and a scholarship to J.I. We thank the Laboratorio de Visualizacion y Computo en Paralelo at UAM-Iztapalapa, DGSCA at UNAM, and NCSA at Illinois for giving us access to their computer facilities. We also thank Laura Escobar for many useful discussions.

JA973762B